Catal Lett
DOI 10.1007/s10562-017-2146-x

MgFeCe Ternary Layered Double Hydroxide as Highly Efficient and Recyclable Heterogeneous Base Catalyst for Synthesis of Dimethyl Carbonate by Transesterification

Nayana T. Nivangune[1] · Vivek V. Ranade[2] · Ashutosh A. Kelkar[1]

Received: 14 February 2017 / Accepted: 9 June 2017

Abstract A series of Mg_3:$Fe_x + Ce_{1-x}$ LDHs (3:1) were synthesized by co-precipitation method by varying molar ratio of Fe:Ce between 1:0 to 0:1 (LDH-1 to LDH-6). All synthesized LDHs were characterized by XRD, FT-IR, TEM, N_2 sorption, benzoic acid titration and XPS in detail and evaluated for selective synthesis of dimethyl carbonate by transesterification of ethylene carbonate with methanol. It was demonstrated that the structural and basic properties of synthesized LDHs were strongly dependent on the Fe:Ce molar ratio (Ce concentration). The correlation between their physicochemical properties and catalytic performance was studied in detail. Among all synthesized LDHs the best result was obtained with LDH-3 (Fe:Ce = 0.85:0.15) where LDH structure remained intact, and showed high number of strong basic sites on LDH surface. LDH-3 was recycled 7 times while maintaining high catalyst activity and selectivity towards DMC. The obtained results elucidate the important role of Ce in modifying the basic properties of LDH in enhancing the catalytic activity for DMC synthesis.

Electronic supplementary material The online version of this article (doi:10.1007/s10562-017-2146-x) contains supplementary material, which is available to authorized users.

✉ Vivek V. Ranade
V.Ranade@qub.ac.uk

✉ Ashutosh A. Kelkar
aa.kelkar@ncl.res.in

[1] Chemical Engineering and Process Development (CEPD) Division, National Chemical Laboratory, Pune 411008, India

[2] School of Chemistry and Chemical Engineering, Queen's University Belfast, Belfast BT9 5AG, Northern Ireland, UK

Published online: 03 August 2017

Graphical Abstract

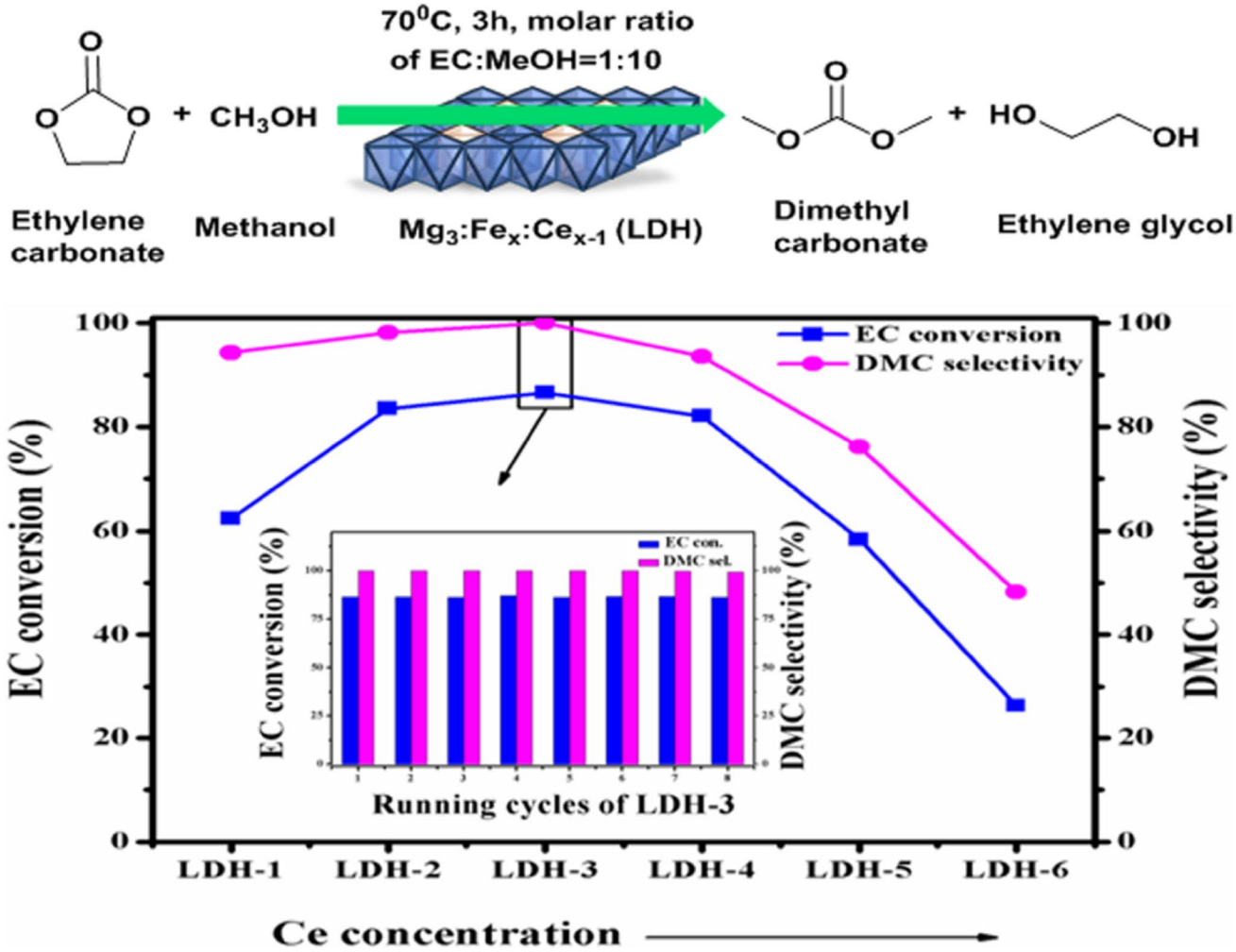

Keywords Dimethyl carbonate · Ethylene carbonate · Mg–Fe–Ce ternary hydrotalcite · Transesterification

1 Introduction

Dimethyl carbonate (DMC) is an important chemical, which gained intense interest from scientific and industrial fields, due to its low toxicity and good biodegradability. DMC is being looked as a green chemical for the production of polycarbonate and other chemicals [1]. It is also used as a safe replacement for toxic phosgene in carbonylation and methylation reactions [2]. In addition DMC has potential applications as electrolyte in lithium batteries as a polar aprotic solvent and as an octane booster in gasoline to meet oxygenate specifications [3–5]. Conventionally DMC was synthesized via phosgenation [6] and presently manufactured by oxidative carbonylation of methanol [7]; both of these routes require corrosive and poisonous gases like chlorine, $COCl_2$ and CO. In case of oxidative carbonylation of methanol there is a risk associated with the explosion hazard of CO/O_2 mixture. One clean and sustainable route for the synthesis of DMC is the transesterification of cyclic carbonate [ethylene carbonate (EC)/propylene carbonate (PC)] with methanol [8]. This is a safe and atom efficient process and ethylene glycol is formed as the by-product. Ethylene glycol is important chemical and also can be converted back to ethylene carbonate by reaction with urea [9]. Significant work is being carried out on the development of improved catalysts for the synthesis of DMC from EC and methanol. Simple inorganic, organic bases and ionic liquids (ILs) were found to be active catalysts for DMC synthesis; still applications are limited because of difficulties in catalyst-product separation due to its homogeneous nature [10–12]. Further Immobilization of the IL on different supports have been explored but high cost of catalyst has limited their application [13, 14]. Considerable amount of work has been carried out on the development of heterogeneous catalysts for the synthesis of DMC. Heterogeneous catalysts based on mixed metal oxides [15–19],

smectite [20], anion-exchange resin [21], Na-dawsonite [22], mesoporous graphitic carbon nitride [23] and Binary hydrotalcites (i.e. LDHs) [24, 25] etc. have been studied for transesterification reaction. Recently Xu et al. reported 78% DMC yield at 160 °C in 6 h with meso structured graphitic carbon nitride (CN-MCF) catalyst [23]. The catalyst was recycled five times without significant loss in catalyst activity; however, harsh reaction conditions (160 °C and 0.6 MPa CO_2 pressure) were necessary to achieve observed results. Among all heterogeneous catalysts investigated mixed metal oxides were found to be active catalysts for this reaction, however, they require either high reaction temperature (100–160 °C) or high catalyst loading (10–25 wt%) [15–18]. The catalyst was recycled four to five times, but catalyst activation at high temperature was required in most of the cases during each recycle experiment. This potentially may cause problem in continuous or large scale operation. In this context it is still challenging task to develop heterogeneous catalysts exhibiting high catalyst activity and high stability for the synthesis of DMC from EC and methanol under mild reaction conditions. Hydrotalcites (HTs) or Layered double hydroxides (LDHs) constitute a class of layered compounds complementary to classic clays, as they contain positively charged layers and anions in the interlamellar space [26]. LDHs are widely studied and successfully used as basic catalysts for several reactions such as condensation, Michael addition, transesterification, and alkylation etc [27]. From the literature it was observed that there are very limited reports on the use of binary LDHs/HTs as catalysts for transesterification of EC with methanol. Bajaj et al. reported that the catalyst activity was influenced by Mg–Al ratio and Mg–Al LDH with molar ratio of 5:1 showed maximum activity [25]. Unfortunately, significant decrease in activity was observed after fourth recycle due to structural changes in catalyst indicating lower stability of the catalyst. According to Watanabe et al. basicity (–OH sites) of LDH plays an important role in this transestrification reaction [24]. Mg–Al LDH with excess amount of –OH anions was found to be an effective catalyst for DMC synthesis. It is well known that basicity of LDH can be tuned by proper choice of M(II) and M(III) metal cations or by varying the molar ratio of M(II)/M(III) [25, 28, 29]. Recently incorporation of third metal cation in parent LDH has attracted much more attention with the aim of modifying basicity of the catalyst. Recently Zhang et al. [30] have reported the synthesis of Mg/Fe + Ce–CO_3 ternary LDH for the first time, however, many important details on characterization are lacking and its catalytic applications have not been investigated.

In this work we have synthesized a series of $Mg_3Fe_xCe_{1-x}$ ternary LDHs, by varying molar ratio of Fe:Ce. All synthesized LDHs were characterized in detail by various spectroscopic techniques. Influence of Ce and its concentration on the properties and catalytic activity of Mg_3: Fe layered double hydroxide ($Mg_3Fe_xCe_{1-x}$) for DMC synthesis (Scheme 1) was investigated in detail. Ceria has lower electronegativity compared to Fe and incorporation of Ce in the Mg_3-Fe LDH could result in increase in the basicity of $Mg_3Fe_xCe_{1-x}$ LDHs and better activity towards DMC synthesis. With this idea in mind the present work on the synthesis of $Mg_3Fe_xCe_{1-x}$ ternary LDHs was initiated. To the best of our knowledge, this is the first report on the use of Ternary LDHs ($Mg_3Fe_xCe_{1-x}$) as a catalyst for the synthesis of DMC from EC and methanol.

2 Experimental

2.1 Catalyst Preparation

A series of $Mg_3Fe_xCe_{1-x}$ LDHs were synthesized by co-precipitation method followed by hydrothermal treatment. The Mg:Fe + Ce molar ratio was kept constant at 3:1; while Fe:Ce molar ratio was varied (1:0 to 0:1). In a typical procedure solution A was prepared by dissolving desired amount of $Mg(NO_3)_2{\cdot}6H_2O$, $Fe(NO_3)_3{\cdot}9H_2O$ and $Ce(NO_3)_3{\cdot}6H_2O$ in deionized water and solution B was prepared by dissolving NaOH and Na_2CO_3 (2 M) in deionized water. Solutions A and B were added simultaneously while pH of the resultant solution was maintained at 10–11 with constant stirring at room temperature. The gel obtained was hydrothermally treated at 90 °C for 15 h. Then the precipitate was filtered, washed several times with deionized water till filtrate became neutral. Finally, the synthesized ternary LDHs were dried at 100 °C for 12 h in air. LDHs prepared with different Fe:Ce molar ratios 1:0, 0.95:0.05, 0.85:0.15, 0.75:0.25, 0.55:0.45, and 0:1 were named as LDH-1, LDH-2, LDH-3, LDH-4, LDH-5 and LDH-6 respectively.

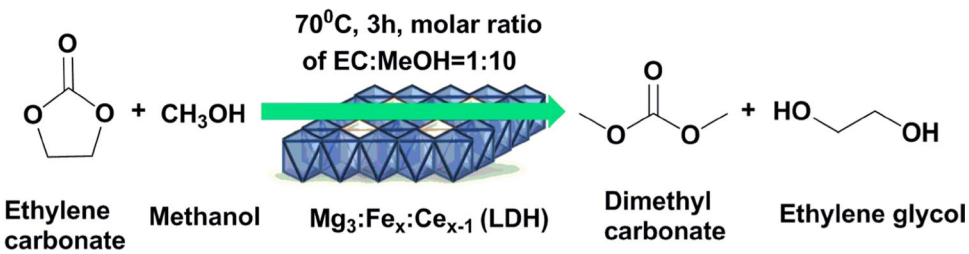

Scheme 1 Schematic diagram of synthesis of dimethyl carbonate from ethylene carbonate and methanol over layered double hydroxide (LDHs)

Elemental chemical compositions of $Mg_3Fe_xCe_{1-x}$ LDHs were determined with the help of ICP-OES method (Table S1). Metal composition in all "neat" LDH samples, was found to be in good agreement with the values based on compositions used for the preparation.

Various ternary $Mg_3Fe_{0.85}M_{0.15}$ LDHs were prepared by same method by varying M(III) [where M(III) = La, Sm, Y and Cr]. See supporting information for the details of synthesis and characterization of $Mg_3Fe_{0.85}M_{0.15}$ LDHs (Page S3).

2.2 Catalyst Characterization

X-ray diffraction (XRD) patterns were recorded on a P Analytical PXRD system (Model X-Pert PRO-1712), using Ni filtered Cu Kα radiation (λ = 0.154 nm) as an X-ray source (current intensity, 30 mA; voltage, 40 kV) and an X-accelerator detector. The samples were scanned in a 2θ range of 10°–80°.

FT-IR spectra were recorded on a Shimadzu 8201 spectrophotometer in 400–4000 cm^{-1} region. The samples were diluted prior to measurement with KBr in a 2/98 mixture ratio.

Transmission electron microscopy (TEM) analysis was performed on a Jeol Model JEM 1200 electron microscope operated at an accelerating voltage of 120 kV. A small amount of specimen was prepared by ultrasonically suspending the powder sample in IPA, and drops of the suspension were deposited on a carbon coated copper grid dried at room temperature before analysis.

The N_2 adsorption–desorption isotherms at −196 °C were obtained using a Thermo surfer BET instrument and the surface areas were deduced using the BET equation. Before analysis, the samples were out gassed at 100 °C for 6 h.

The basic properties were determined by titration with 0.01 M benzoic acid solution in toluene using 0.15 g of vacuum dried solid sample suspended in 2 mL of indicator solution. Indicator solution for the determination of weak basic sites (pKa = 7.1) contained 0.01 g of bromothymol blue in 100 mL toluene. The amount of strong basic sites (pKa = 9.3) were determined in the presence of an indicator solution containing 0.01 g of Phenolphthalein in 100 mL toluene [31, 32].

XPS spectra were recorded on a VG Microtech Multilab ESCA3000 spectrometer equipped with non-monochromatised Mg-Kα radiations (hv = 1253.6 eV).

2.3 Catalytic Tests

The transesterification of ethylene carbonate with methanol over the Ce incorporated ternary LDHs was performed in a 50 ml jacketed glass reactor equipped with magnetic stirrer and reflux condenser. Typically, the reactor was charged with 23 mmol of ethylene carbonate, 230 mmol of methanol and 2.5 wt% of LDH catalyst (relative to EC). The reaction was carried out at 70 °C for 3 h reaction time under vigorous stirring. After 3 h of the reaction, the glass reactor was cooled to room temperature; the solid catalyst was separated from the solution by filtration. Sample was analyzed by gas chromatography to monitor the progress of the reaction. The gas chromatograph (Agilent 6890N) was equipped with an FID detector and an innowax capillary column (30 m length × 0.53 mm × ID 0.25 µm film thickness). Formation of HEMC (2-hydroxy ethyl methyl carbonate, intermediate product), DMC and EG as products were confirmed by GC-MS. Activity of the catalyst was based on conversion of limiting reagent under standard reaction conditions. Stability and leaching of LDHs was investigated under optimized reaction conditions (Page S4).

3 Results and Discussion

3.1 Powder X-ray Diffraction

The XRD patterns of all synthesized ternary $Mg_3Fe_xCe_{1-x}$ LDHs with different Fe:Ce molar ratios are shown in Fig. 1. LDH-1 to LDH-3 showed typical features of highly crystalline LDH materials with an R3m rhombohedral space group symmetry [33, 34]. No other phase was detected in these samples indicating that cerium species are successfully incorporated into LDHs. Nevertheless, with increase in Ce concentration for LDH-4 to LDH-6 decrease in crystallinity (better ordering of brucite sheets) which is directly proportional to the peak intensity and sharpness of (003) and (006) planes; was observed. This is due

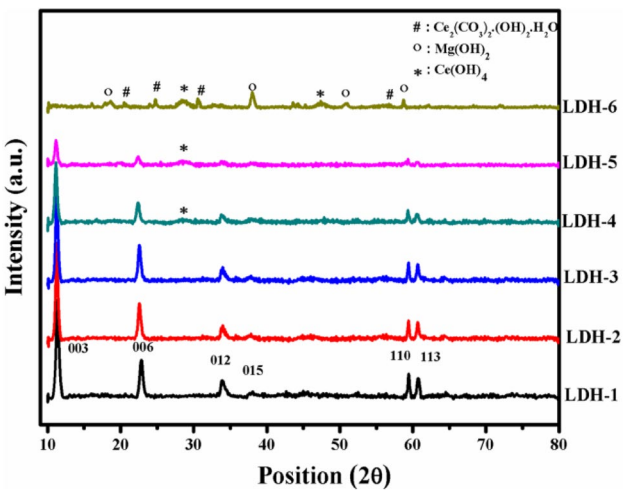

Fig. 1 XRD patterns of all synthesized $Mg_3Fe_xCe_{1-x}$ LDHs (LDH-1 to LDH-6)

to the substitution of Fe (0.65 Å) by larger ionic radii of Ce (1.01 Å), which inhibits the intercalation of Ce in LDH structure and also leads to significant distortion in the layers [35]. At higher Ce concentration (LDH-6, Fe:Ce = 0:1) the layered structure collapsed completely and formation of phases like $Mg(OH)_2$ (PCPDF-86-0441), $Ce(OH)_4$ [36, 37] and $Ce_2(CO_3)_2{\cdot}(OH)_2{\cdot}H_2O$ (PCPDF-46-0369) was observed. The lower electronegativities of rare earth elements (REEs), could favour formation of these species at the initial stage of precipitation [38].

The lattice parameters 'a' and 'c' were calculated and are summarized in Table 1.

Parameter 'a' ($a = 2d_{110}$) depends mainly on the average radius of the metal cation and reflected the density of metal ions in 110 plane. [35] The observed results may be due to the isomorphous substitution of Fe by Ce having larger ionic radii [39]. Thus more Ce insertion leads to an increase in average radius of cations in the layers and this leads to increase in 'a' parameter.

Parameter 'c' ($c = 3d_{003}$) depends on the thickness of octahedral sheets, the anion size and their orientation within the interlayer space and the electrostatic attraction between different layers [40]. Lower polarizing ability of the Ce results in weak electrostatic interaction between the layer and interlayer anions and leads to increase in the layer spacing resulting in increase of the 'c' parameter value. Thus increase in values of parameters 'a' and 'c' with increase in Ce concentration (Table 1, LDH-1 << LDH-5) may be attributed to larger ionic radii and lower polarizing ability of Ce [39, 40].

3.2 FT-IR Spectroscopy

The FT-IR spectral information can be used to determine the actual bonding type in the expected compounds and to determine the substitution of Ce in the brucite layer. FT-IR spectra of all LDH samples (Fig. 2) showed broad band centered around 3500 cm^{-1} due to the stretching mode of hydroxyl groups present in the brucite-like layers and from the interlayer water molecules of the hydrotalcite structure. The band at 3681 cm^{-1} was observed in LDH-4 << LDH-6; which is characteristic of non-hydrogen bound –OH group [41]. A weaker band at 1630 cm^{-1} is owing to the bending mode of water molecules. IR absorption bands at 1510 cm^{-1}, 1382 cm^{-1} (υ_3), 852 cm^{-1} (υ_2), and 1056 cm^{-1} (υ_1) are attributed to the carbonate anion environment [42, 43]. The bands recorded in the low-frequency region of the spectrum (<700 cm^{-1}) are assigned to the translational mode of M–O–H and M–OH–M vibrations. Significant difference in these bands was observed with an increase in Ce concentration of synthesized LDHs. The FT-IR spectra of the LDH-1 to LDH-3 showed the typical bands of the hydrotalcite-like compounds [42]. In case of LDH-4 to LDH-6 a new band was observed at 3681 cm^{-1}, which corresponds to non bonded –OH group vibrations for $M(OH)_x$.

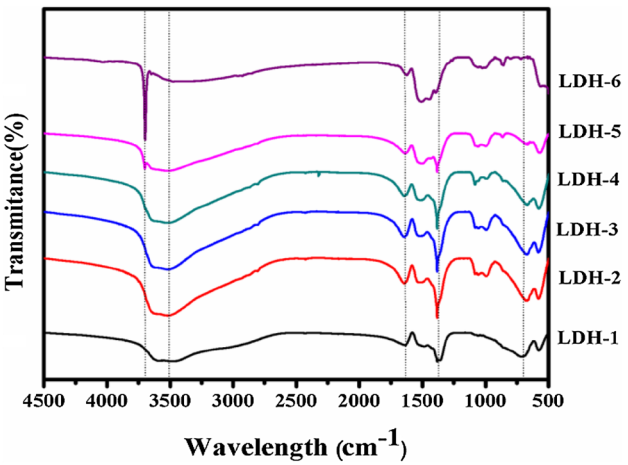

Fig. 2 FT-IR spectra of synthesized $Mg_3Fe_xCe_{1-x}$ LDHs

Table 1 Characteristics of the prepared samples

Sample	Lattice parameters (Å)				Surface area (m^2/g)	Pore volume (cm^3/g)	Pore diameter (nm)	Basic sites ($\times10^{-4}$ mol/g)	
	d(003)	d(110)	a	c				Weak basic sites	Strong basic sites
LDH-1	7.78	1.566	3.112	23.34	67	0.51	16.8	1.8	1
LDH-2	7.85	1.564	3.128	23.55	128	0.8	23	2.4	1.2
LDH-3	7.88	1.572	3.144	23.64	136	0.81	24.3	2.8	1.3
LDH-4	7.92	1.576	3.152	23.76	134	0.78	22.7	3.0	1.0
LDH-5	7.93	1.577	3.154	23.79	133	0.76	21.6	3.5	0.8
LDH-6	nd	nd	nd	nd	129	0.73	20.2	4.5	0.5

nd not detected

3.3 Transmission Electron Microscopy

The influence of Ce concentration on the crystal shape and size was clearly observed from the morphology of all synthesized materials (Fig. 3). The TEM images (Fig. 3A–C) showed that the LDHs (LDH-1 to LDH-3) are composed of crystallites with the typical plate like morphology and often hexagonal shaped [39]. However, in LDH-4 and LDH-5 (Fig. 3D, E) particles of irregular shape with agglomerated small particles of $[Ce(OH)_4]$ on surface and edges of crystallites were observed. In case of LDH-6 (Fig. 3F) the layered structure was absent with significant increase in agglomerated particles. The crystalline nature of the individual materials (LDH-1 to LDH-6) was further checked by selected area electron diffraction (SAED) patterns shown in the Fig. 3(A–F). LDH-1 to LDH-3 samples showed good crystalline nature which decreased with increase in Ce concentration (LDH-4 to LDH-6) [44].

3.4 Surface Area Measurements

BET surface areas and textural properties of catalysts were determined by nitrogen adsorption–desorption isotherms and the values obtained are summarized in Table 1. The BET surface area, pore volume and pore size increased with increase in Ce concentration from LDH-1 to LDH-3. LDH-3 showed nearly two times more surface area (136 m^2/g) than parent LDH-1 (67 m^2/g). With further increase in Ce content from LDH-4 to LDH-6; slight decrease in surface area and pore volume was observed. This may be due to (1) distortion in layer structure because of incorporation of excess amount of Ce, (2) deposition of the agglomerated particles formed during precipitation conditions or their incorporation into the pore system of LDH respectively [45].

3.5 Basicity Measurement

The nature of the active species present on the surface is important for establishing the properties of the catalyst. Consequently, basic properties of the catalysts were determined by benzoic acid titration of the basic sites in the presence of pH indicators and the results are presented in Table 1. The strong basic sites correspond to –OH sites present in brucite like structure and weak basic sites correspond to carbonate species and simple metal bonded –OH group $[M(OH)_x]$ present in synthesized materials [46, 47]. From the Table 1 it can be clearly observed that the weak basic sites increased consistently with increase in Ce concentration LDH-1 to LDH-6. However strong basic sites increased with increase in Ce concentration from LDH-1 to LDH-3 and decreased with further increase

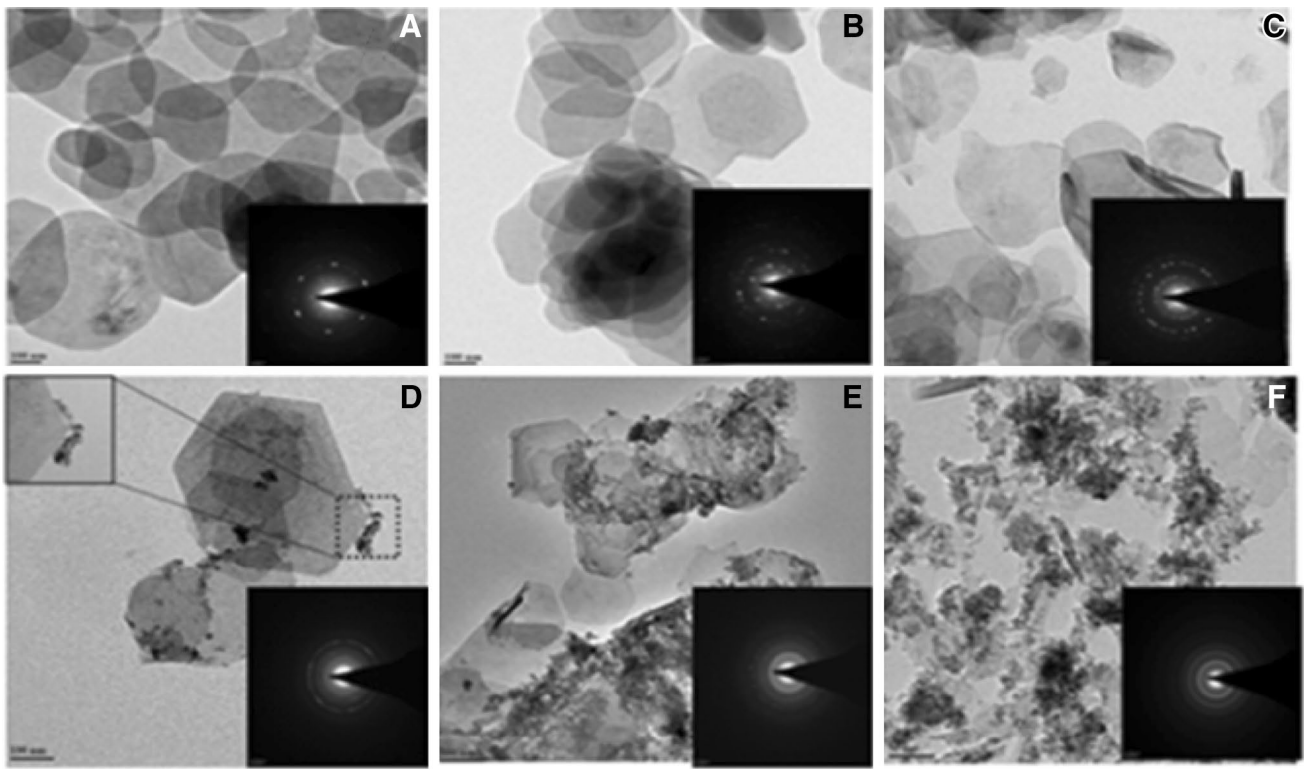

Fig. 3 TEM images and SAED patterns of synthesized $Mg_3Fe_xCe_{1-x}$ LDHs **A** LDH-1, **B** LDH-2, **C** LDH-3, **D** LDH-4, **E** LDH-5 and **F** LDH-6

in Ce concentration for LDH-4 to LDH-6. Parent LDH-1 has less number of strong and weak basic sites than Ce incorporated LDHs (LDH-2 and LDH-3). The increase in basic properties and also the increase in surface area for Ce incorporated LDHs (LDH-2 and LDH-3) can be correlated to exchange of Fe with Ce having lower electronegetivity [39].

3.6 X-ray Photoelectron Spectroscopy

The XPS spectra of Ce 3d and O1s have been analyzed in detail (see Supporting Information pages S5–S7), in order to understand the effect of Ce concentration on surface active sites (–OH) of synthesized LDHs. Figure S2 shows the XPS spectra of Ce 3d for the synthesized LDHs (LDH-2 to LDH-5). XPS spectra of the Ce 3d core level can be resolved into 10 groups; and the representative example of the fitting procedure for the Ce3d of LDH-6 is presented in Fig. 4 [48]. The Ce 3d spectrum of all samples (LDH-2–LDH-6) indicated presence of mixed valence states of Ce^{3+} and Ce^{4+}. The peaks attributed to O 1s are observed at 530.6 and 532.3 eV (Fig. S3). The first one, with a very low intensity is characteristic of O^{2-} (attributed to carbonate species) designated as ''O_β'', whereas the high intensity second peak corresponds to the oxygen species in hydroxide form (–OH) designated as ''O_α'' [49]. The quantitative analysis of the Ce 3d and O1s XPS peaks for the samples is summarized in Table S2 and includes percentage concentrations of the Ce^{4+}, Ce^{3+}, O_α and O_β species present on the material surface. From the Table S2 it was clearly observed that the gradual increase in Ce^{4+} concentration has taken place from LDH-4 to LDH-6 (60.2–69.1%) with increase in Ce concentration. This indicates that increase in Ce concentration has led to increase in Ce^{4+} present on the surface in the form of $Ce(OH)_4$. The amount of Ce in LDH structure also affects the concentration of surface O_α and O_β (Table S2). Parent compound (LDH-1) has surface O_α concentration of 78.3% and increased with Ce loading for materials having LDH structure intact (86.9% for LDH-2 and 87.2% for LDH-3). Further increase in ceria concentration (LDH-4 to LDH-6) led to marginal drop in the concentration of surface O_α (85.2–81.6%) with rise in O_β (14.3–18.4%). Probably with increase in Ce concentration (LDH-4 to LDH-6) the distortion in the layer structure occurred; which led to marginal decrease in surface O_α group and relatively O_β species are exposed to the sample surface.

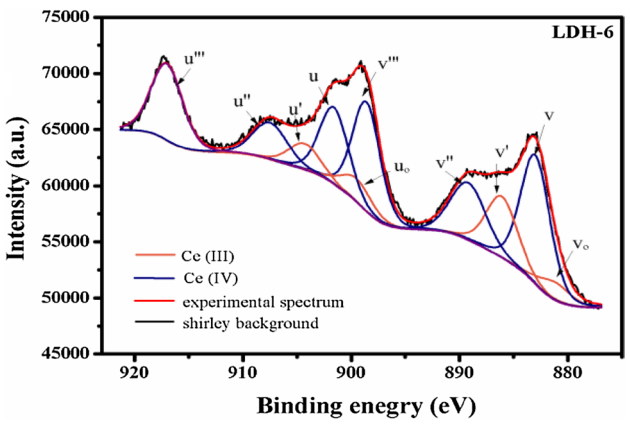

Fig. 4 Representative example of the fitting procedure for the Ce 3d peak of LDH-6

The detailed characterization results demonstrate that the structural, textural and chemical properties of the LDHs can be fine-tuned by doping with appropriate amount of another trivalent metal such as Ce. XRD, FT-IR and TEM analysis (Figs. 1, 2, 3) clearly showed that LDH-1 to LDH-3 formed well defined LDH structure with high crystallinity (better ordering of brucite sheets). No other phase was detected, implying that Ce was well incorporated in the prepared LDHs. Among which LDH-3 showed high surface area and pore volume with high amount of strong basic sites present on LDH surface (Table 1). Further with increase in Ce concentration (LDH-4 to LDH-6) distortion in layer structure was observed from XRD, TEM and XPS analysis. This may be due to the isomorphic substitution of Fe by large ionic radii cation Ce. In case of LDH-4 and LDH-5 precipitation of $Ce(OH)_4$ on surface was clearly observed and confirmed by XRD, TEM and FT-IR analysis. LDH structure was totally absent for LDH-6 (Fe:Ce = 0:1) and mixed hydroxide, carbonate phases were observed. These observations are found to be consistent with surface area, pore volume and strong basic site densities (hydroxyl groups present in the brucite-like structure) of LDHs, which marginally decreased from LDH-4 to LDH-6. Distortion in LDH structure results in the decrease in surface area, pore volume and structure bonded –OH groups (strong basic sites). According to literature reports, the structure bonded –OH group are strong basic in nature than simple metal bonded –OH groups ($Mg(OH)_2$ or $Ce(OH)_4$) [46, 47]. The decrease in the intensity of FT-IR band at 3500 cm^{-1} (–OH) for LDH-4 to LDH-6 (Fig. 2); also supports this observation. Characterization of the catalysts indicated that layered structure was intact till LDH-3 and LDH-3 was found to be material with higher surface area, pore volume and higher amount of strong basic sites.

3.7 Catalyst Activity

Ce promoted $Mg_3Fe_xCe_{1-x}$ LDHs were investigated for the transesterification reaction and the results are presented in Fig. 5. From the results, it was clearly observed that catalyst activity trend is in the order of LDH-6 < LDH-5 < LDH-1 < LDH-4 < LDH-2 < LDH-3.

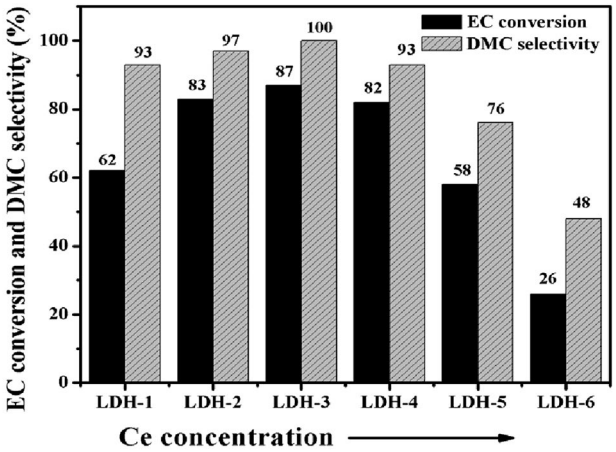

Fig. 5 Effect of Ce concentration in $Mg_3Fe_xCe_{1-x}$ LDHs towards the transesterification reaction. Reaction conditions: EC: 23 mmol, EC: MeOH molar ratio: 1:10, catalyst: 2.5 wt% relative to EC, reaction time: 3 h, temperature: 70 °C

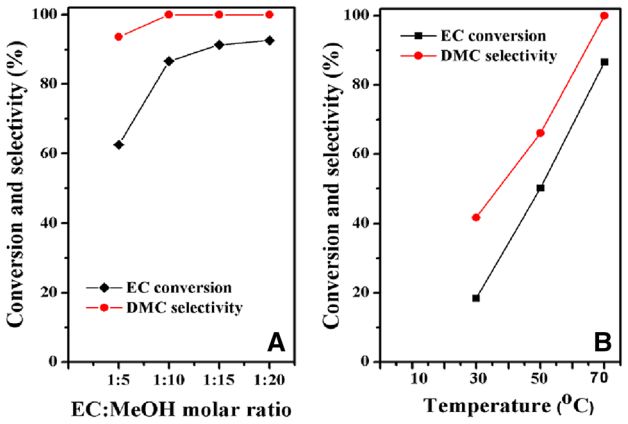

Fig. 6 Effect of EC:MeOH molar ratio (**A**) and reaction temperature (**B**) on the catalytic transesterification. Reaction conditions: **A** EC: 23 mmol, EC: MeOH: 1:5–1:20, catalyst: 2.5 wt% relative to EC, reaction time: 3 h, temperature: 70 °C. **B** EC: 23 mmol, EC: MeOH: 1:10, catalyst: 2.5 wt% relative to EC, reaction time: 3 h, temperature: 30–70 °C

Catalyst activity increased with increase in Ce concentration up to a level and decreased with further increase in Ce concentration. Among all synthesized catalysts LDH-3 showed maximum EC conversion (87%) and DMC selectivity (100%). It should be noted that both binary systems LDH-1 (Mg_3:Fe) and LDH-6 (Mg_3:Ce) were found to be less active as compared to LDH-3 (EC conversion 62 and 26% with DMC selectivity 93 and 48% respectively). Thus the activity observed was strongly dependent on the Ce concentration in the synthesized LDHs. The observed activity trend was found to be in good agreement with physicochemical properties of synthesized LDHs. Thus, EC conversion was lower with LDH-1 and increased with Ce concentration (LDH-2 < LDH-3). Best results were obtained with LDH-3 ($Mg_3Fe_{0.85}Ce_{0.15}$) having highest amount of strong base sites present on LDH surface with high surface area and pore volume as compared to other LDHs. With further increase in Ce concentration (LDH-4–LDH-6) strong basic sites, surface area and pore volume decreased and could be attributed to the formation and deposition of $Ce(OH)_4$ phase and distorted nature of layered structure of LDHs; which reduced the catalyst activity. This is in accordance with the results obtained by Kannan et al. for hydroxylation of phenol using CoNiAl ternary LDH as catalyst [50]. They concluded that strong basic sites (hydroxyl groups) play an important role in catalytic activity and the appropriate geometry and concentration of both the metal cations in a well ordered two dimensional lattice could be responsible for the activity observed. The most active catalyst (LDH-3) was taken for further study. Effect of EC/CH_3OH molar ratio on the transesterification reaction was investigated using LDH-3 catalyst (Fig. 6A). From Fig. 6A it was clearly observed that the EC/CH_3OH feed molar ratio had a significant impact on the transesterification reaction. Transesterification of EC and methanol (EC + MeOH ⇌ DMC + EG) is an equilibrium controlled reaction and hence excess methanol is required to shift the equilibrium towards right and achieve high selectivity to DMC as the product [16–19]. EC conversion (63–87%) and DMC selectivity (92–100%) increased gradually with increase in the feed molar ratio of EC /CH_3OH from 1:5 to 1:10. Further increase in EC/CH_3OH ratio from 1:15 to 1:20 had marginal effect on EC conversion (92–94%) with 100% selectivity to DMC. The effect of reaction temperature (30–70 °C) also has a significant impact on the activity and selectivity of the reaction. Thus at 30 °C EC conversion of 18% with 43% selectivity to DMC was observed. EC conversion and DMC selectivity increased with increase in temperature and 51% conversion of EC with 66% selectivity to DMC was observed at 50 °C. Low selectivity to DMC was because of the formation of HEMC as major product. Results indicate that higher temperature as well as higher EC:methanol mole ratio are necessary for the conversion of intermediate HEMC to DMC. Zhang et al. [12] also have observed similar results in the transesterification of EC and methanol using carboxylic functionalized imidazolium salt as the catalyst. Best results (87% EC conversion and 100% DMC selectivity) were obtained at 70 °C. The effect of catalyst loading is presented in Fig. 7. Activity was low at a catalyst loading of 0.6 wt% and 72% conversion of EC with 93% selectivity to DMC was observed. Activity and selectivity to DMC increased with catalyst loading and 87% conversion of EC with 100% selectivity to DMC was observed at a catalyst loading of 2.5 wt%. The improved performance

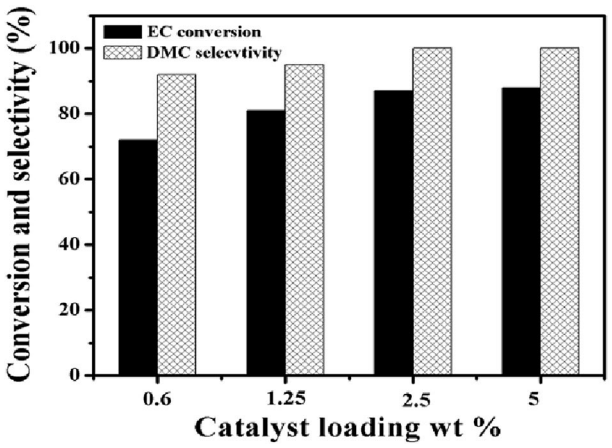

Fig. 7 Effect of catalyst loading on transesterification of EC with methanol using LDH-3. Reaction conditions: EC: 23 mmol, EC: MeOH: 1:10, catalyst: 0.6–5 wt% relative to EC, reaction time: 3 h, temperature: 70 °C

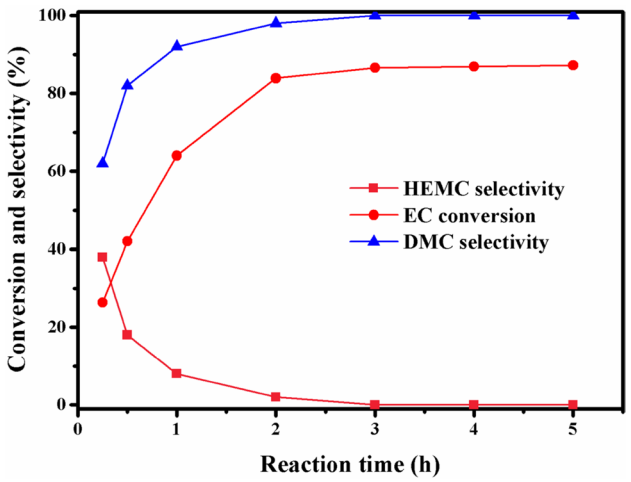

Fig. 8 Effect of reaction time on EC conversion and DMC selectivity. Reaction conditions: EC: 23 mmol, EC: MeOH: 1:10, catalyst: 2.5 wt% relative to EC, reaction time: 0.5–5 h, temperature: 70 °C

observed with increase in catalyst loading can be attributed to increase in basic sites available for the reaction. Further increase in catalyst loading (2.5–5 wt%) had marginal effect on EC conversion (87–89%) showing high selectivity to DMC (100%). Catalyst loading of 2.5 wt% was taken as optimum for this reaction and used for further study.

All the experiments in this study were carried out with sampling in a time range of 1–5 h. However, since the data is exhaustive; the detailed parametric study data with results at different time intervals is presented in supporting information (Figs. S4–S6).

Finally typical conversion/selectivity vs time plot under optimized reaction conditions using LDH-3 catalyst is presented in Fig. 8. EC conversion and DMC selectivity increased, while HEMC selectivity decreased with increase in reaction time. Maximum EC conversion (87%) and DMC selectivity (100%) was observed at 3 h reaction time. Further prolonging the reaction time had no positive effect on EC conversion indicating that the reaction has reached the equilibrium [17]. Lower selectivity of DMC observed at intermediate time intervals is due to the formation of HEMC as intermediate product.

After optimization of reaction conditions with $Mg_3Fe_{0.85}Ce_{0.15}$ (LDH-3) it was decided to investigate the effect of incorporation of other trivalent metals (instead of Ce) on the performance of the catalyst. For this purpose LDHs were prepared by varying M(III) [where M(III) = La, Sm, Y and Cr] by keeping the molar ratio of 3:0.85:0.15 constant and tested for transesterification of EC with methanol under identical reaction conditions. From the Table 2 it was clearly observed that doping of different trivalent metal cations in parent LDH-1 (Mg_3:Fe) affected the EC conversion and DMC selectivity significantly. Activity and selectivity followed in the order of $La \approx Ce > Sm > Y > Cr$. Among all LDHs $Mg_3Fe_{0.85}Ce_{0.15}$ (LDH-3) showed best activity and selectivity for this reaction. The results were found to be consistent with the electro negativities of the metal cations ($1.1 \approx 1.12 < 1.17 < 1.22 < 1.66$ respectively). Incorporation of third cation which has low electronegativity results in the increase in basic property of LDH and leads to better activity [37]. The difference in the electronegativities of La and Ce is very small and expectedly the catalyst activities observed were comparable. Thus Ce incorporated Mg_3:Fe LDH was found to be best catalyst for transesterification reaction.

3.8 Catalyst Stability

To check the stability of the catalyst recycle experiments were carried out and the results are presented in Fig. 9. It was observed that the catalyst retained its original activity

Table 2 Effect of different metal cation Mg_3:$Fe_{0.85}$:$M_{0.15}$ for transesterification reaction of EC with MeOH

Catalyst	EC conversion (%)	DMC selectivity (%)
Mg_3:Fe_1	62	94
Mg_3:$Fe_{0.85}$:$La_{0.15}$	85	99
Mg_3:$Fe_{0.85}$:$Ce_{0.15}$	87	100
Mg_3:$Fe_{0.85}$:$Sm_{0.15}$	81	95
Mg_3:$Fe_{0.85}$:$Y_{0.15}$	67	82
Mg_3:$Fe_{0.85}$:$Cr_{0.15}$	56	78

Reaction conditions: EC: MeOH molar ratio: 1:10, catalyst: 2.5 wt% relative to EC, reaction time: 3 h, temperature: 70 °C.

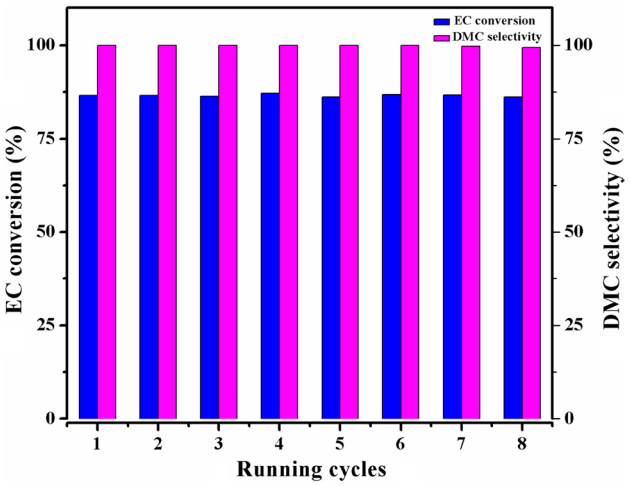

Fig. 9 Catalyst recycles study, reaction conditions: EC: 23 mmol, EC: MeOH: 1:10, catalyst: 2.5 wt% relative to EC, reaction time: 3 h, temperature: 70 °C

and selectivity for seven recycle experiments indicating excellent stability. Further to check whether the catalyst leached out in reaction mixture; reaction was carried out by hot filtration and the results are summarized in the Fig. S7.

It was found that in the absence of the catalyst, there was no further increase in the EC conversion, which indicated that there was no leaching and transesterification is purely a heterogeneously catalyzed reaction. At the end of the 7 recycle experiments the XRD analysis of the used catalyst was carried out (Fig. S8). No change in the XRD pattern was observed for used catalyst, indicating high stability of the catalyst (LDH-3) towards transeserification reaction. From the literature it was observed that mixed metal oxides were active catalysts for DMC synthesis and high reaction temperature (100–180 °C) and catalyst loading (10–25 wt% of EC) was required in these cases [15–17]. The catalysts were stable up to 4–5 recycle experiments; however activation of the recovered catalyst at higher temperature was necessary before each reuse. Ternary $Mg_3Fe_{0.85}Ce_{0.15}$ (LDH-3) catalyst developed in the present work does not require any pre-treatment and could be recycled up to seven times without loss in EC conversion and DMC selectivity under mild reaction conditions.

3.9 Catalytic Mechanism

Mechanism of the transeterification of EC with methanol has been discussed in several reports [11, 23, 25]. Hydroxy groups (strong basic sites) present on LDH surface play an important role in transesterification reaction which was studied by many researchers using various spectroscopic techniques. According to Roeffaers et al. transesterification of 5-carboxyfluorescein with 1-butanol over [Li–Al] layered double hydroxide catalyst occurs on the basal planes of the outer crystal surface whereas the hydrolysis reaction takes place on the crystal edges [51]. Additionally, Greenwell et al. have presented evidence form density functional theory (DFT) calculations that surface bonded –OH anion may directly participate in the catalytic reaction and act more than the simple metal hydroxyl group [52]. In the present work, significant improvement in EC conversion was observed with incorporation of Ce in the Mg_3-Fe LDH (LDH-3). Detailed characterization of the catalyst indicated the presence of more amount of active sites (-OH group) on LDH surface with high surface area compared to parent Mg_3-Fe LDH (LDH-1). Taking into account the literature reports and results observed in the present work a probable mechanism has been proposed (scheme 2); where the –OH species and metal cations present above the LDH surface act as strong base and Lewis acid sites respectively.

The reaction begins with the abstraction of proton from methanol on –OH sites of LDH to generate methoxy anion and activation of carbonyl carbon of EC on Lewis acid sites of LDHs to generate relatively charged carbonyl carbon (step I). Generated methoxy anion attacks on the activated carbonyl carbon of EC to form HEMC as the intermediate product (step II). In next step (III) another methanol molecule will attack in similar fashion to form DMC and EG as the final products and the catalyst is regenerated back (step IV). The formation of HEMC as an intermediate product was observed at low EC: CH_3OH ratios (Fig. 6A) and at low reaction temperature (Fig. 6B) leading to poor selectivity to the target DMC.

4 Conclusions

Transesterification of EC with methanol to DMC was investigated in detail using $Mg_3Fe_xCe_{1-x}$ ternary LDH as the catalyst. The LDHs were synthesized by varying Fe:Ce molar ratio in a range of 1:0–0:1. Both the end members of this series Mg_3Fe (LDH-1) and Mg_3Ce (LDH-6) showed lower catalytic activity and selectivity to DMC. The significant increase in EC conversion and DMC selectivity was observed with appropriate concentration of Ce present in LDH structure. The activity varied in the order LDH-6 < LDH-5 < LDH-1 < LDH-4 < LDH-2 < LDH-3. Among the synthesized catalysts LDH-3 (Fe:Ce molar ratio: 0.85:0.15) showed best catalytic performance (87% EC conversion with 100% DMC selectivity) under mild reaction conditions. LDH-3 was found truly heterogeneous catalyst and was recycled seven times without loss in catalytic activity and selectivity to DMC. The activity trend was found to be in good agreement with structural and surface basic properties of the synthesized LDHs. Various trivalent metals were also used to modify the LDH with composition

Scheme 2 A possible mechanism for the transesterification of ethylene carbonate with methanol catalyzed by LDH-3

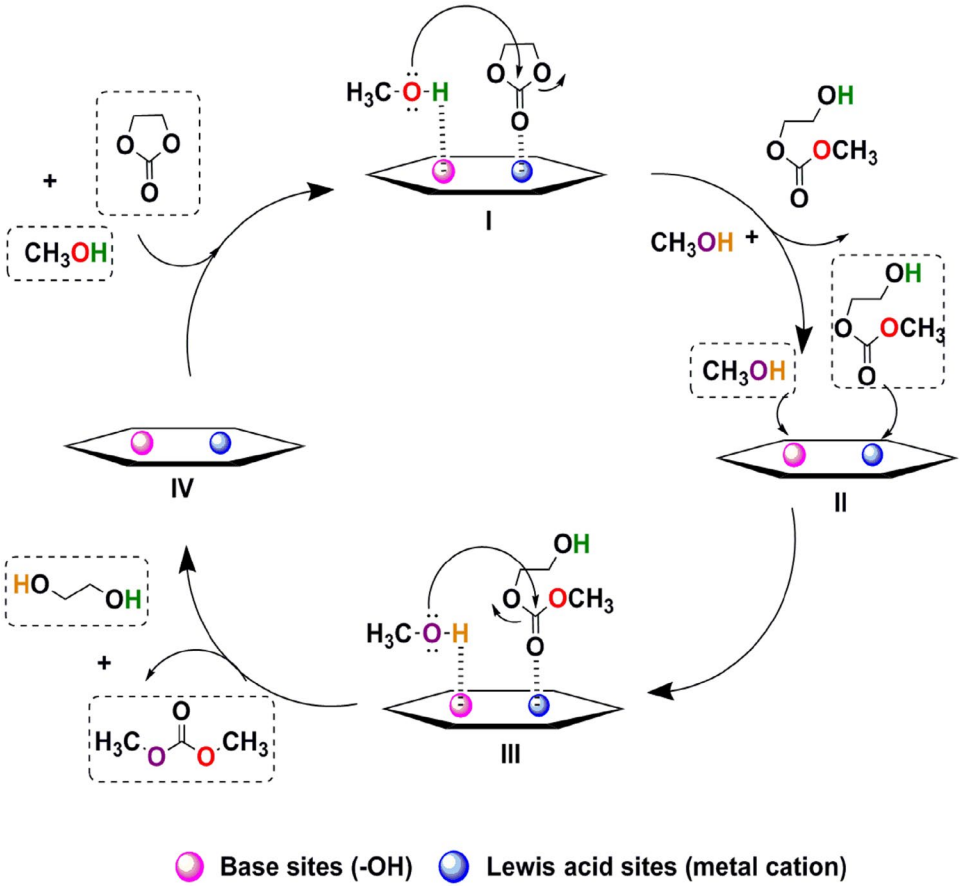

$Mg_3Fe_{0.85}M_{0.15}$ [where M(III) = La, Sm, Y and Cr] and the activity trend followed in order of La ≈ Ce > Sm > Y > Cr. The best results were obtained with Ce modified Mg_3:Fe LDH ($Mg_3Fe_{0.85}Ce_{0.15}$) as the catalyst. The results were found to be in good agreement with the electronegativities of incorporated third metal cations [M(III)]. To the best of our knowledge this is the first report on the use of $Mg_3Fe_{0.85}Ce_{0.15}$ ternary LDH as a catalyst for this reaction.

Acknowledgements Authors would like to acknowledge partial financial support to the work from the project CSC0123 funded by CSIR-Delhi, India. NTN would like to acknowledge CSIR-Delhi, India for fellowship grant.

References

1. Huang S, Yan B, Wang S, Ma X (2015) Chem Soc Rev 44:3079
2. Tundo P, Selva M (2002) Acc Chem Res 35:706
3. Shaikh AAG, Sivaram S (1996) Chem Rev 96:951
4. Pacheco MA, Marshall CL (1997) Energy Fuels 11:2
5. Rounce P, Tsolakis A, Leung P, York APE (2010) Energy Fuels 24:4812
6. Babad H, Zeiler AG (1973) Chem Rev 73:75
7. Drake IJ, Fujdata KL, Bell AT (2005) J Catal 230:14
8. Fukuoka S, Tojo M, Hachiya H, Aminaka M, Hasegawa K (2007) Polym J 39:91
9. Fakhrnasova D, Chimento RJ, Medina F, Urakawa A (2015) ACS Catal 5:6284
10. Du GF, Guo H, Wang Y, Li WJ, Shi WJ, Dai B (2015) JSaudi Chem Soc 19:112
11. Yang ZZ, Dou XY, Chanfreau SB (2010) Tetrahedron Lett 51:2931
12. Zhang SJ, Wang JQ, Sun J, Cheng WG, Shi CY, Dong K, Zhang XP (2012) Catal Sci Technol 2(5):600
13. Xu J, Wu HT, Ma CM, Xue B, Li YX, Cao Y (2013) Appl Catal A 464:357
14. Kim DW, Lim DO, Cho DH, Koh JC, Park DW (2011) Catal Today 164:556
15. Bhanage BM, Fujita SI, Ikushima Y, Arai M (2001) Appl Catal A 219:259
16. Murugan C, Bajaj HC (2013) Indian J Chem 52A:459
17. Kumar P, Srivastava VC, Mishra IM (2015) Energy Fuels 29:2664
18. Unnikrishnan P, Srinivas D (2015) J Mol Catal A 398:42
19. Sankar M, Satav S, Manikandan P (2010) ChemSusChem 3:575
20. Bhanage BM, Fujita SI, Ikushima Y, Torii K, Arai M (2003) Green Chem 5:71
21. Tatsumi T, Watanabe Y, Koyano KA (1996) Chem Commun 19:2281
22. Stoica G, Abello SN, Perez-Ramirez J (2009) Appl Catal A 365:252
23. Xu J, Long KZ, Chen T, Xue B, Li YX, Cao Y (2013) Catal Sci Technol 3:3192

24. Watanabe Y, Tatsumi T (1998) Microporous Mesoporous Mater 22:399
25. Murugan C, Bajaj HC (2010) Indian J Chem 49A:1182
26. Cavani F, Trifiro F, Vaccari A (1991) Catal Today 11:173
27. Nishimura S, Takagaki A, Ebitani K (2013) Green Chem 15:2026
28. Cantrell DG, Gillie LJ, Lee AF, Wilson K (2005) Appl Catal A 287:183
29. Jana SK, Wu P, Tatsumi T (2006) J Catal 240:268
30. Liu Z, Li L, Chen Y, Zhang Y (2014) Acta Geol Sin 88:354
31. Malinowski S, Szczepaoska S (1963) J Catal 2:310
32. Zavoianu R, Birjega R, Pavel OD, Cruceanu A, Alifanti M (2005) Appl Catal A 286:211
33. Triantafyllidis KS, Peleka EN, Komvokis VG, Mavros PP (2010) J Colloid Interface Sci 342:427
34. Peng F, Luo T, Yuana Y (2014) New J Chem 38:4427
35. Wang D, Zhang X, Ma J (2016) Catal Sci Technol 6(5):1530
36. Tang K, Zhang J, Wang W, Wang S, Guo J, Yang Y (2015) CrystEngComm 17:2690
37. Ansari AA, Kaushik A (2010) J Semicond 31:033001
38. Wang Z, Fongarland P, Lu G, Essayem N (2014) J Catal 318:108
39. Pavel OD, Cojocaru B, Angelescu E (2011) Appl Catal A 403:83
40. Zhao Y, Li JG, Fang F, Chu N, Ma H, Yang X (2012) Dalton Trans 41:12175
41. Caravaggio GA, Detellier C, Wronski Z (2001) J Mater Chem 11:912
42. Jun H, Zhiliang Z, Hongtao L, Yanling Q (2014) RSC Adv 4:5156
43. Perez MR, Crespo I, Ulibarri MA, Barriga C, Rives V, Fernandez JM (2012) Mater Chem Phys 132:375
44. Baliarsingh N, Mohapatra L, Parida K (2013) J Mater Chem A 1:4236
45. Wang D, Zhang X, Ma J, Yu H, Shena J, Wei W (2015) Catal Sci Technol 6:1530
46. Navajas A, Campo I, Arzamendi G, Hernajndez WY, Bobadilla LF, Centeno MA, Odriozola JA, Gandia LM (2010) Appl Catal B 100:299
47. Xi Y, Davis RJ (2008) J Catal 254:190
48. Hu Z, Liu X, Meng D, Guo Y, Guo Y, Lu G (2016) ACS Catal 6:2265
49. Parida K, Satpathy M, Mohapatra L (2012) J Mater Chem 22:7350
50. Rives V, Prieto O, Dubey A, Kannan S (2003) J Catal 220:161
51. Roeffaers MBJ, Sels BF, Uji-i H, De Schryver FC, Jacobs PA, Hofkens J (2006) Nature 439:572
52. Greenwell HC, Stackhouse S, Coveney PV, Jones W (2003) J Phys Chem B 107:3476